International Journal of Engineering & Technology, 7 (4.41) (2018) 50-54

International Journal of Engineering & Technology

Website: www.sciencepubco.com/index.php/IJET

Research paper

Numerical Scheme Based on Operational Matrices for Integro-Differential Equations

C. S. Singh[1], A. K. Singh[2], J.K. Sahoo[3]*

[1]*Department of Mathematics, IIT(BHU), Varanasi, India*
[2]*Department of Mathematics, IIT Madras, Chennai, India*
[3]*Department of Mathematics, BITS Pilani K K Birla Goa Campus, Goa, India*
**Corresponding author E-mail:jksahoo@goa.bits-pilani.ac.in*

Abstract

An effective numerical tool based on wavelets and orthogonal polynomials are presented for the solution of a class of system of singular Voltera integro-differential equations (SSVIDEs). We also presented the convergence analysis for the derivative of the approximation in terms of Legendre wavelets. In this paper, we propose a numerical wavelet and polynomial methods for solving SSVIDEs of second kind. The method is based on the operational and almost operational matrix of integration based on wavelet and orthogonal polynomials. We use the concept of operation matrix of integration to convert the main problem into linear system of algebraic equations. Some numerical examples along with error evaluation are given to illustrate the accuracy and efficiency of the proposed method. The advantage of the proposed technique is computationally most simple, low cost of setting the algebraic equations without using artificial smoothing factors.

Keywords: *Legendre wavelets, Bernstein polynomials, Operational matrices, Singular voltera integro-differential equations.*

1. Introduction

System of singular Voltera integro-differential equations (SSVIDEs) arises in many branches of science and engineering such as biological models electromagnetic, fluid dynamics, financial economics, heat and mass transfer etc. The main application of system of integro-differential equations (SIDEs) in Wilson-Cowan model [11,12] which describes the evolution of excitatory and inhibitory activity in a coupled neuronal network. In 1997, first Amari [1] gave the following mathematical expression for the Wilson-Cowan model:

$$\frac{\partial E}{\partial t} = -E + \int w_{ee}(x-x')f(E-\theta_1)dx' - \int w_{ie}(x-x')f(E-\theta_2)dx' + \psi_1(x,t)$$

$$\tau\frac{\partial I}{\partial t} = -I + \int w_{ei}(x-x')f(E-\theta_1)dx' - \int w_{ii}(x-x')f(E-\theta_2)dx' + \psi_2(x,t),$$

With initial conditions $E(x,0) = E_0(x), I(x,0) = I_0(x)$ and $x \in \mathbb{R},\ t \geq 0$. Here $E(x,t)$ and $I(x,t)$ represents the activity of a population of excitatory and inhibitory neurons respectively. The function w_{ij} describes the strength of connection from cell type k to j and f is firing rate function or some case Heaviside function. The positive parameters θ_1, θ_2 and τ denotes the inhibitory time constant, threshold levels for E and I respectively. ψ_1 and ψ_2 are external inputs. Pinto and Ermentrout [9,10] modified the Wilson-Cowan model as the following:

$$\frac{\partial u}{\partial t} = -u - v + \int w(x-x')H(u-\theta)dx'$$

$$\tau\frac{\partial v}{\partial t} = \epsilon(\beta u - v),$$

where u is the activity excitatory neurons and v could represent spike frequency adaption, synaptic depression or some other slow process that the excitation of the network. Existence of solutions to the above systems using topological shooting and Evans function method already discussed in [2].In this article, we will not discuss exactly the numerical solutions of Wilson-Cowan model but in general to SSVIDEs. Singh et.al.[3,4] have developed numerical schemes for integro-differential equations(IDEs) using operational matrix concepts based on wavelets and orthogonal polynomial approximations as well. System of Voltera integro-differential equations (SVIDEs) mainly for non-singular and linear type using hybrid functions, Haar wavelets and Runge-Kutta methods are discussed in [5, 6, 7]. In [8], numerical solution of singular Volterra integral equations (SVIEs) system of convolution type by using operational matrices also considered. Though all are gives approximation solutions only some discussed about analytical solution by restricting the function in some extent. In this paper, we promote and analyze the mess-less scheme based on Legendre wavelet operational matrices and Berstein polynomials operational matrices for solving the following SSVIDEs.

$$\sum_{j=1}^{2} a_{ij} D^{\alpha} y_j = \sum_{k=1}^{2} b_{ik} f_k(x) + \lambda_i \sum_{l=1}^{2} \int_0^x \frac{c_{il} y_i(t)}{\sqrt{x-t}} dt \qquad (1)$$

with initial conditions $y_i(0) = d_i$, where $i = 1,2$. We assume that the functions $f_1(x)$ and $f_2(x)$ are square integrable functions.

2. Operational matrices

2.1. Bernstein polynomials and operational matrices

The Bernstein basis polynomials of degree n form a complete basis over the interval $[0,1]$ are defined by

$$B_{j,n}(t) = \binom{n}{j} t^j (1-t)^{n-j} \quad \text{for } j = 0,1,\dots,n. \tag{2}$$

Where t is a parameter. However, the Bernstein basis polynomials can be generalized to cover an arbitrary interval $[a, b]$ by normalizing t over the interval $[a, b]$,i.e. $t = \frac{(x-a)}{(b-a)}$, which lead to the following

$$B_{j,n}(t) = \binom{n}{j} \frac{(x-a)^j (b-x)^{n-j}}{(b-a)^n} \quad \text{for } j = 0,1,\dots,n. \tag{3}$$

These polynomials satisfy symmetry$B_{j,n}(x) = B_{n-j,n}(1-x)(x)$, positivity $B_{j,n}(x) \geq 0$, form a partition of unity $\sum_{j=0}^{n} B_{j,n}(x) = 1$ on the defining interval $[a, b]$. The explicit representation of the orthogonal Bernstein basis polynomials, denoted by $\hat{B}(x) = \phi_{j,n}(x)$ and it is obtained by using Gram-Schmidt orthonormalization process on . If function $f \in L^2[0,1]$,then

$$f(t) = \lim_{n\to\infty} \sum_{j=0}^{n} c_{jn}\, \hat{b}_{jn}(t). \tag{4}$$

Here $c_{jn} = < f, \hat{b}_{jn} >$, where $<,>$ is the inner product over $L^2[0,1]$. If the series (4) is truncated at $n = m$, then denote

$$f(t) \approx \sum_{j=0}^{m} c_{jn}\, \hat{b}_{jn}(t) = C^T \hat{B}(t), \tag{5}$$

Where $C = [c_{0m}, c_{1m}, \cdots, c_{mm}]^T$, $\hat{B}(t) = [\hat{b}_{0m}, \hat{b}_{1m}, \cdots, \hat{b}_{mm}]^T$. In this case the orthonormal Bernstein polynomials operational matrix of integration and almost operational matrix of integration of order $(m+1) \times (m+1)$ are given respectively by

$$\int_0^x \hat{B}(t)dt = P_6^B \hat{B}(x) \tag{6}$$

and

$$\int_0^x \frac{\hat{B}(t)}{\sqrt{x-t}} dt = S_6^B \hat{B}(x). \tag{7}$$

For $n = 5$ the explicit expressions for P_6^B and S_6^B via five orthonormal polynomials for (6) and (7) are presented in the articles[13,14,15]respectively.

2.2. Legendre wavelets polynomials and operational matrices

The Legendre wavelet basis functions Ψ_{nm} are defined as follows

$$\Psi_{nm}(t) = \begin{cases} \sqrt{2m+1}\, 2^{k/2} P_m(2^k t - \hat{n}), & \text{for } \frac{\hat{n}-1}{2^n} \leq t < \frac{\hat{n}+1}{2^n}, \\ 0, \text{otherwise}, \end{cases} \tag{8}$$

where $P_m(t)$ are Legendre polynomials of degree m defined on $[-1,1]$ by the following recurrence relation for $m = 1,2,3,\dots$:

$P_0(t) = 1, P_1(t) = t$ and $P_{m+1}(t) = \frac{2m+1}{m+1} t P_m(t) - \frac{m}{m+1} P_{m-1}(t)$.

The other arguments take the values within the following range: $\hat{n} = 2n-1,\ n = 1,\ 2,\ 3,\dots,2^{k-1},\ k = 1,\ 2,\ 3,\dots,m$.

A function $g(x)$ defined over $[0,1]$ may be expanded by the Legendre wavelets as:

$$g(x) = \sum_{n=1}^{\infty} \sum_{m=0}^{\infty} C_{nm}\, \Psi_{nm}(x), \tag{9}$$

where $C_{nm} = < g, \Psi_{nm} >$. and $<,>$ is the inner product on $L^2[0,1]$. If the infinite series (9) is truncated, then it can be written as

$$g(x) \approx \sum_{n=1}^{2^{k-1}} \sum_{m=0}^{M} C_{nm}\, \Psi_{nm}(x) = C^T \Psi(x), \tag{10}$$

where the matrices C and Ψ are given by ,

$C = [C_{10}, C_{11}, \cdots, C_{1M}, C_{20}, C_{21}, \cdots, C_{2M}, \cdots, C_{2^{k-1}0}, \cdots, C_{2^{k-1}M}]$ and

$\Psi(x) = [\Psi_{10}, \Psi_{11}, \cdots, \Psi_{1M}, \Psi_{20}, \Psi_{21}, \cdots, \Psi_{2M}, \cdots, \Psi_{2^{k-1}0}, \cdots, \Psi_{2^{k-1}M}]$.

Similarly Legendre wavelets operational matrix of integration are defined as $(2^{k-1}M) \times (2^{k-1}M)$ are denoted by

$$\int_0^x \Psi(t)dt = P_6^L \Psi(x) \tag{11}$$

and

$$\int_0^x \frac{\Psi(t)}{\sqrt{x-t}} dt = S_6^L \Psi(x) \tag{12}$$

The explicit expressions for the Legendre wavelet functions and operational matrices can be found in [16,17] for $M = 3$ and $k = 2$.

3. Mess-less scheme derivation

Consider the system of singular Voltera integro-differential equation (1) and considering the orthogonal approximation of both known functions $f_1(x)$ and $f_2(x)$ as

$$f_1(x) \simeq F_1^T \Phi(x) \text{ and } f_2(x) \simeq F_2^T \Phi(x), \tag{13}$$

where $\Phi(x) = [\Phi_0(x), \Phi_1(x), \Phi_2(x), \Phi_3(x), \Phi_4(x), \Phi_5(x)]^T$ and $\Phi_0(x), \Phi_1(x), \Phi_2(x), \Phi_3(x), \Phi_4(x)$, and $\Phi_5(x)$ are orthogonal polynomials in the interval (0,1]. Also $F_i = [F_{i0}, F_{i1}, F_{i2}, F_{i2}, F_{i4}, F_{i5}]^T$ for $i = 1$ and 2. The components are determined by the given expression:

$F_{ij} = \int_0^1 f_i(x)\Phi_j(x)dx, \quad 0 \leq j \leq 5.$

We let the approximation for the derivative term as

$$\frac{dy_1}{dx} \simeq C_1^T \Phi(x) \text{ and } \frac{dy_2}{dx} \simeq C_2^T \Phi(x). \tag{14}$$

Integrating the equation (14) from 0 to x, we obtain

$y_1(x) - a = C_1^T \int_0^x \Phi(x)dx$ and $y_2(x) - b = C_2^T \int_0^x \Phi(x)dx$.

We assume $a \simeq A^T \Phi(x) = A_0\Phi_0 + A_1\Phi_1 + A_2\Phi_2 + A_3\Phi_3 + A_4\Phi_4 + A_5\Phi_5$ and $b \simeq B^T \Phi(x) = B_0\Phi_0 + B_1\Phi_1 + B_2\Phi_2 + B_3\Phi_3 + B_4\Phi_4 + B_5\Phi_5$ where $A_i = \int_0^1 a\,\Phi_i(x)dx$ and $B_i = \int_0^1 b\,\Phi_i(x)dx \quad 0 \leq i \leq 5$.

By using approximation for the integral $\int_0^x \Phi(x) = P\Phi(x)$, and the above expressions we have

$$y_1(x) \simeq A^T \Phi(x) + C_1^T P\Phi(x) \text{ and } y_2(x) \simeq B^T \Phi(x) + C_2^T P\Phi(x). \tag{15}$$

Applying $y_1(x), \frac{dy_2}{dx}$, and the approximation $\int_0^x \frac{\Phi(x)}{\sqrt{x-t}} \simeq S\Phi(x)$ in equation (1), we get

$$C_1^T\left(a_{11}\Phi(x) - a_{15}PS\Phi(x)\right) + C_2^T\left(a_{12}\Phi(x) - a_{16}PS\Phi(x)\right) = a_{13}F_1^T\Phi(x) + a_{14}F_2^T\Phi(x) + a_{15}A^T S\Phi(x) + a_{16}B^T S\Phi(x) \tag{16}$$

Since $\Phi(x)$ is non zero function, we can write equation (16) as

$$C_1^T(a_{11}I_{6\times6} - a_{15}PS) + C_2^T(a_{12}I_{6\times6} - a_{16}PS) = a_{13}F_1^T + a_{14}F_2^T + a_{15}A^TS + a_{16}B^TS \quad (17)$$

Similarly from the second equation of the system (1), we have the following equation

$$C_1^T(a_{21}I_{6\times6} - a_{25}PS) + C_2^T(a_{22}I_{6\times6} - a_{26}PS) = a_{23}F_1^T + a_{24}F_2^T + a_{25}A^TS + a_{26}B^TS \quad (18)$$

By solving equation (17) and (18) for C_1^T, C_2^T, we obtain:

$$C_1^T = [(a_{13}F_1^T + a_{14}F_2^T + a_{15}A^TS + a_{16}B^TS)(a_{12}I_{6\times6} - a_{16}PS)^{-1} - (a_{23}F_1^T + a_{24}F_2^T + a_{25}A^TS + a_{26}B^TS)(a_{22}I_{6\times6} - a_{26}PS)^{-1}] \times [(a_{11}I_{6\times6} - a_{15}PS)(a_{12}I_{6\times6} - a_{16}PS)^{-1} - (a_{21}I_{6\times6} - a_{25}PS)(a_{22}I_{6\times6} - a_{26}PS)^{-1}]^{-1}$$

$$C_2^T = [(a_{13}F_1^T + a_{14}F_2^T + a_{15}A^TS + a_{16}B^TS)(a_{11}I_{6\times6} - a_{15}PS)^{-1} - (a_{23}F_1^T + a_{24}F_2^T + a_{25}A^TS + a_{26}B^TS)(a_{21}I_{6\times6} - a_{25}PS)^{-1}] \times [(a_{12}I_{6\times6} - a_{16}PS)(a_{11}I_{6\times6} - a_{15}PS)^{-1} - (a_{22}I_{6\times6} - a_{26}PS)(a_{21}I_{6\times6} - a_{25}PS)^{-1}]^{-1}.$$

Substituting the value of C_1^T and C_2^T in equation (15) we can get the approximated numerical solution $y_1(x)$ and $y_2(x)$ for the system (1).

Table 1: The List of Notations.

General symbols: $\Phi(x)$, P, S, F_1, F_2, A, y_1, y_2, C_1^T, C_2^T.
Usage of Legedre polynomials: $\psi_{nm}(x)$, P_6^L, S_6^L, F_1^L, F_2^L, A_6^L, y_1^L, y_2^L, $C_1^{T,L}$, $C_2^{T,L}$.
Usage of Bernstein polynomials: $\hat{B}(x)$, P_6^B, S_6^B, F_1^B, F_2^B, A_6^B, y_1^B, y_2^B, $C_1^{T,B}$, $C_2^{T,B}$

4. Convergence analysis

Theorem 4.1. Suppose that the function $D^\alpha y_M(x)$ obtained by using Legendre wavelets are the approximation of $D^\alpha y(x)$ and $D^\alpha y(x)$ and its second derivative is bounded, then we have the following upper bound of error $\| D^\alpha y(x) - D^\alpha y_M(x) \|_E^2 \le \frac{A^2}{2^{k+1}} F_3(-1/2 + M)$ where, $\|y(x)\|_E = (\int_0^1 |y(x)|^2 dx)^{1/2}$, $D = \frac{d}{dx}$ and A is positive constant.

Proof. Let $D^\alpha y(x) = \sum_{n=0}^{\infty}\sum_{m=0}^{\infty} C_{nm}\Psi_{nm}(x)$, $D^\alpha y_M(x) = \sum_{n=1}^{2^{k-1}}\sum_{m=0}^{M} C_{nm}\Psi_{nm}(x)$, where $D^\alpha y_M(x)$ be the following approximation of $D^\alpha y(x)$. Grouping the above two equations, we get $D^\alpha y(x) - D^\alpha y_M(x) = \sum_{n=(2^{k-1}+1)}^{\infty}\sum_{m=(M+1)}^{\infty} C_{nm}\Psi_{nm}(x)$.

Let $D^\alpha y(x)$ be a function defined on $[0,1)$ such that $|D^{\alpha+2}y(x)| \le A$, where A is a positive constant. Since $\{\psi_{nm}(x)\}$ are orthonormal on $[0,1)$ so we have $\int_0^1 \psi_{nm}(x)\psi_{nm}(x)^T dx = I$, where I is identity matrix.

$$\| D^\alpha y(x) - D^\alpha y_M(x) \|_E^2 = \int_0^1 (D^\alpha y(x) - D^\alpha y_M(x))^2 dx = \int_0^1 (\sum_{n=(2^{k-1}+1)}^{\infty}\sum_{m=(M+1)}^{\infty} C_{nm}\Psi_{nm}(x))^2 dx = \sum_{n=(2^{k-1}+1)}^{\infty}\sum_{m=(M+1)}^{\infty} C_{nm}^2.$$

Where $C_{nm} = \langle D^\alpha y(x), \Psi_{nm}(x)\rangle$

$$= \int_0^1 D^\alpha y(x)\Psi_{nm}(x)dx = \int_{\hat{n}-1}^{\hat{n}+1} D^\alpha y(x)(2m+1)^{1/2}2^{k/2}P_m(2^kx - \hat{n})dx$$

$$= \frac{(2m+1)^{1/2}2^{k/2}}{2^k}\int_{\hat{n}-1}^{\hat{n}+1} D^\alpha y(x)P_m(2^kx - \hat{n})dx = \frac{(2m+1)^{1/2}2^{k/2}}{2^k}\int_{-1}^{1} D^\alpha y(x)P_m(t)dt$$

$$= \frac{(2m+1)^{1/2}2^{k/2}}{2^k}\int_{-1}^{1} D^\alpha y(x)d\left(\frac{P_{m+1}(t) - P_{m-1}(t)}{2m+1}\right)dt$$

$$= \left[\frac{1}{2^k(2m+1)}\right]^{\frac{1}{2}}\int_{-1}^{1} D^\alpha y(x)d(P_{m+1}(t) - P_{m-1}(t))dt$$

$$= -\left[\frac{1}{2^k(2m+1)}\right]^{\frac{1}{2}}\int_{-1}^{1} D^{\alpha+1} y(x)(P_{m+1}(t) - P_{m-1}(t))dt$$

$$= -\left[\frac{1}{2^k(2m+1)}\right]^{\frac{1}{2}}\int_{-1}^{1} D^{\alpha+1} y(x)d\left(\frac{P_{m+2}(t) - P_m(t)}{2m+3} - \frac{P_m(t) - P_{m-2}(t)}{2m-1}\right)dt$$

$$= \left[\frac{1}{2^k(2m+1)}\right]^{\frac{1}{2}}\int_{-1}^{1} D^{\alpha+1} y(x)d\left(\frac{P_{m+2}(t) - P_m(t)}{2m+3} - \frac{P_m(t) - P_{m-2}(t)}{2m-1}\right)dt.$$

Thus

$$|C_{nm}|^2 \text{ and } \frac{1}{2^k(2m+1)}\left|\int_{-1}^{1} D^{\alpha+2} y(x)\left(\frac{(2m-1)P_{m+2}(t) - (4m+2)P_m(t) + (2m+3)P_{m-2}(t)}{(2m+3)(2m-1)}\right)dt\right|^2$$

$$\le \frac{1}{2^k(2m+1)}\int_{-1}^{1} |D^{\alpha+2}y(x)|^2\int_{-1}^{1}\left|\left(\frac{(2m-1)P_{m+2}(t) - (4m+2)P_m(t) + (2m+3)P_{m-2}(t)}{(2m+3)(2m-1)}\right)\right|^2 dt$$

$$\le \frac{A^2}{2^k(2m+1)}\int_{-1}^{1}\left|\left(\frac{(2m-1)P_{m+2}(t) - (4m+2)P_m(t) + (2m+3)P_{m-2}(t)}{(2m+3)(2m-1)}\right)\right|^2 dt$$

$$< \frac{A^2}{2^k(2m+1)}\int_{-1}^{1}\left|\left(\frac{(2m-1)^2P^2_{m+2}(t) + (4m+2)^2P^2_m(t) + (2m+3)^2P^2_{m-2}(t)}{(2m+3)^2(2m-1)^2}\right)\right|dt$$

$$= \frac{A^2}{2^k(4m^2-1)(2m-1)(2m+3)}\left[\frac{2(2m-1)^2}{2m+5} + \frac{8(2m+1)^2}{2m+1} + \frac{2(2m+3)^2}{2m-3}\right] < \frac{3A^2}{2^{k-2}(2m-3)^4}.$$

Therefore, $\sum_{m=M+1}^{\infty} C_{nm}^2 < \sum_{m=M+1}^{\infty}\frac{3A^2}{2^{k-2}(2m-3)^4}$

$$= \frac{3A^2}{2^{k-2}}\sum_{m=M+1}^{\infty}\frac{1}{(2m-3)^4} = \frac{3A^2}{2^{k-2}}\left(\frac{1}{96}\right)F_3\left[\frac{-1}{2} + M\right] = \frac{A^2}{2^{k+1}}F_3\left[\frac{-1}{2} + M\right]$$

Finally, we get $\| D^\alpha y(x) - D^\alpha y_M(x) \|_E^2 \le \frac{A^2}{2^{k+1}}F_3\left[\frac{-1}{2} + M\right]$.

Theorem 4.2. Let f be a real valued function defined, and bounded by M on the interval $[0,1]$. For each point x of continuity of f, $B_n(f)(x) \to f(x)$ as $n \to \infty$. If f is continuous on $[0,1]$, then the Bernstein polynomial $B_n(f)$ tends uniformly to f as $n \to \infty$. With x a point of differentiability of f, $B_n'(f)(x) \to f'(x)$ as $n \to \infty$. If f is continuously differentiable on $[0,1]$ then $B_n'(f)$ tends to f' uniformly as $n \to \infty$. For proof see[18].

5. Numerical examples

In this section we consider the proposed method to find the numerical solution of equation (1) and equation (2).Taking the $\alpha = 1$ and initial condition $y_1 = 0$ and $y_2 = 0$, with the coefficients $a_{11} = 1$, $a_{12} = -1$, $b_{11} = 1$, $b_{12} = 0$, $c_{11} = 1$, $c_{12} = 1$, $\lambda_1 = 1$ $a_{21} = -1$, $a_{22} = -2$, $b_{21} = 0, b_{22} = 1$, $c_{21} = 1$, $c_{22} = 1$. $\lambda_2 = 1$. In each graphs $E1L(t)$ and $E1B(t)$ are errors corresponding to the function Y_1 by using Legendre wavelets and Bernstein polynomials. $E2L(t)$ and $E2B(t)$ are errors corresponding to the function Y_2 by using Legendre wavelets and Bernstein polynomials. The accuracy of the proposed method is demonstrated by calculating, for $i = 1,2$ the parameters of errors $E_i(t)$, average deviation σ_i also known as root mean square error (RMS). They are calculated using the following equations:

$E_i(t)$= Approximate solutions $(y_i(t))$ - Exact solutions $(Y_i(t))$

and

$$\sigma_i = \left\{\frac{1}{N}\sum_{i=0}^{N}[(y_i(t)) - (Y_i(t))]\right\}^{1/2} = \| E_i(t) \|_{l^2}$$

Where $y_i(t)$ and $Y_i(t)$ are the approximate and exact values calculated at points t_j. Note that σ_i is discrete l^2-norm of the error E_i denoted by $\| E_i \|_{l^2}$. We, also, compute the continuous L^2-norm of the error E_i by

$$\| E_i(t) \|_{L^2} = [\int_0^1 E_i^2(t)]^{1/2}.$$

In table 2 and 3, $\| E_i \|_{L^2}^L$ and $\| E_i \|_{L^2}^B$ are continuous error norms using Legendre wavelet and Bernstein polynomial for $i = 1,2$. Similarly $\| E_i \|_{l^2}^L$ and $\| E_i \|_{l^2}^B$ are discrete error norms using Legendre wavelet and Bernstein polynomial for $i = 1,2$.

Example 1.

We have chosen $f_1 = \frac{3}{2}t^{1/2} - 2t - \left(\frac{3\pi t^2}{8} + \frac{16t^{5/2}}{15}\right)$ and $f_2 = -\frac{3}{2}t^{1/2} + 4t - \frac{16t^{5/2}}{15}$ so that exact solutions for equation (1) and equation (2) given by $Y_1 = t^{3/2}$ and $Y_2 = t^2$. The approximate solutions using Legendre wavelets and Bernstein polynomials are given by equation (4) with coefficients.

$C_1^{T,L} = [0.5001 \quad 0.1729 \quad -0.03206 \quad 0.9151 \quad 0.08936 \quad -0.0038]$
$C_2^{T,L} = [0.3535 \quad 0.2039 \quad -0.0001 \quad 1.0611 \quad 0.2042 \quad 0.0001]$
$C_1^{T,B} = [0.2813 \quad 0.5086 \quad 0.5253 \quad 0.5073 \quad 0.4088 \quad 0.2456]$
$C_2^{T,B} = [0.1571 \quad 0.4269 \quad 0.5768 \quad 0.6133 \quad 0.5394 \quad 0.3297]$
$C_1^{T,L} P_6^L(x) = [0.1005 \quad 0.0742 \quad 0.0111 \quad 0.4658 \quad 0.1323 \quad 5.7685]$
$C_2^{T,L} P_6^L(x) = [0.0589 \quad 0.0510 \quad 0.0131 \quad 0.4125 \quad 0.1531 \quad 0.0131]$
$C_1^{T,B} P_6^B(x) = [0.0373 \quad 0.1357 \quad 0.2317 \quad 0.2774 \quad 0.2618 \quad 0.1647]$
$C_2^{T,B} P_6^B(x) = [0.0193 \quad 0.0888 \quad 0.1850 \quad 0.2517 \quad 0.2542 \quad 0.1656]$

Therefore, the approximate solutions corresponding to Legendre wavelets and Bernstein polynomials are given as:

$$y_1^L(x) = C_1^{T,L} P_6^L(x)\psi_{nm}(x), \quad y_2^L(x) = C_2^{T,L} P_6^L(x)\psi_{nm}(x),$$
$$y_1^B(x) = C_1^{T,B} P_6^B(x)\tilde{B}(x), \text{ and } y_2^B(x) = C_2^{T,B} P_6^B(x)\tilde{B}(x).$$

Example 2.

We have chosen $f_1 = -\frac{4}{15}t^{\frac{3}{2}}(-5+8t) - 1$ and $f_2 = 1 - 2t - \frac{16t^{5/2}}{15}$ so that exact solutions for equation (1) and equation (2) given by $Y_1 = t(t-1)$ and $Y_2 = t^2$. The approximate solutions using Legendre wavelets and Bernstein polynomials are given by equation (4) with coefficients.

$C_1^{T,L} = [-0.3535 \quad 0.2041 \quad 0 \quad 0.3535 \quad 0.2041 \quad 0]$
$C_2^{T,L} = [0.3535 \quad 0.2041 \quad 0 \quad 1.0606 \quad 0.2041 \quad 0]$
$C_1^{T,B} = [-0.3960 \quad -0.0739 \quad 0.1343 \quad 0.2383 \quad 0.2480 \quad 0.1611]$
$C_2^{T,B} = [0.1572 \quad 0.4270 \quad 0.5770 \quad 0.6137 \quad 0.5399 \quad 0.3301]$
$C_1^{T,L} P_6^L(x) = [-0.1178 \quad -0.051 \quad 0.0131 \quad -0.1178 \quad 0.051 \quad 0.0131]$
$C_2^{T,L} P_6^L(x) = [0.0589 \quad 0.05103 \quad 0.0131 \quad 0.4124 \quad 0.1530 \quad 0.0131]$
$C_1^{T,B} P_6^B(x) = [-0.05952 \quad -0.1255 \quad -0.1051 \quad -0.0577 \quad -0.0186 \quad -0.0015]$
$C_2^{T,B} P_6^B(x) = [0.0193 \quad 0.0889 \quad 0.1851 \quad 0.2518 \quad 0.2544 \quad 0.1657]$

Therefore, the approximate solutions corresponding to Legendre wavelets and Bernstein polynomials are given as:

$$y_1^L(x) = C_1^{T,L} P_6^L(x)\psi_{nm}(x), \quad y_2^L(x) = C_2^{T,L} P_6^L(x)\psi_{nm}(x),$$
$$y_1^B(x) = C_1^{T,B} P_6^B(x)\tilde{B}(x), \text{and } y_2^B(x) = C_2^{T,B} P_6^B(x)\tilde{B}(x).$$

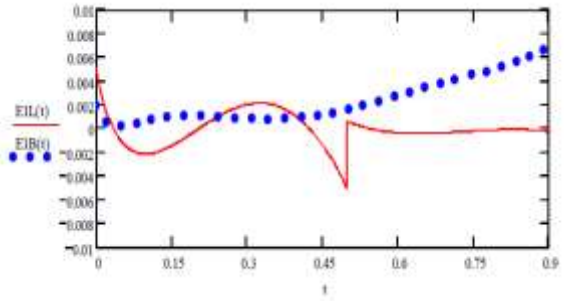

Figure 1: Comparison of approximation errors for the $y_1(t)$ by using Legendre wavelets (solid line) and Bernstein polynomials (dotted line) in case of example 1.

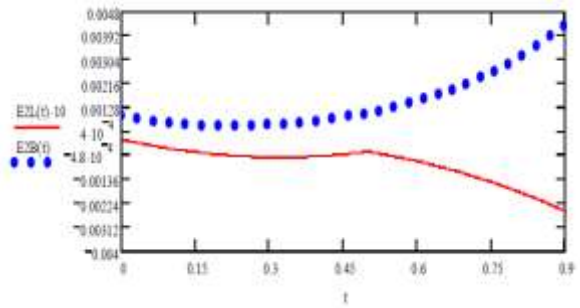

Figure 2: Comparison of approximation errors for the $y_1(t)$ by using Legendre wavelets (solid line) and Bernstein polynomials (dotted line) in case of example 2.

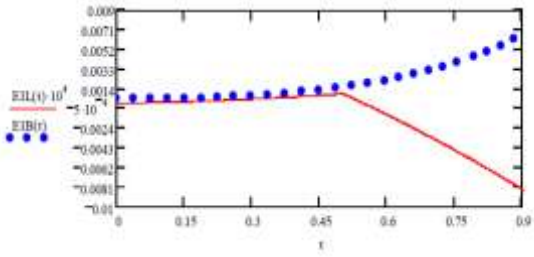

Figure 3: Comparison of approximation errors for the $y_2(t)$ by using Legendre wavelets (solid line) and Bernstein polynomials (dotted line) in case of example 1.

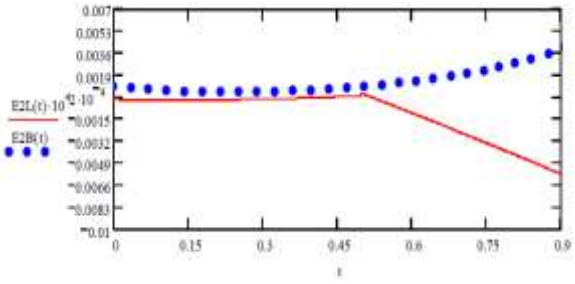

Figure 4: Comparison of approximation errors for the $y_2(t)$ by using Legendre wavelets (solid line) and Bernstein polynomials (dotted line) in case of example 2.

Table 2: The continuous and discrete error norms for $y_1(t)$.

Error norms	Example 1	Example 2
$\| E_1 \|_{L^2}^L$	1.33×10^{-3}	4.17×10^{-7}
$\| E_1 \|_{L^2}^B$	3.92×10^{-3}	3.49×10^{-3}
$\| E_1 \|_{l^2}^L$	3.17×10^{-2}	4.12×10^{-7}
$\| E_1 \|_{l^2}^B$	3.93×10^{-3}	3.50×10^{-3}

Table 3: The continuous and discrete error norms for $y_2(t)$.

Error norms	Example 1	Example 2
$\| E_2 \|_{L^2}^L$	1.33×10^{-4}	2.87×10^{-7}
$\| E_2 \|_{L^2}^B$	2.31×10^{-3}	2.08×10^{-3}
$\| E_2 \|_{l^2}^L$	3.16×10^{-2}	3.16×10^{-2}
$\| E_2 \|_{l^2}^B$	2.31×10^{-3}	2.08×10^{-3}

6. Conclusion

The main aim of this paper was to demonstrate that the wavelet mess-less approximation method is a powerful numerical tool than the orthogonal polynomial mess-less approximation for solving SSVIDEs. The computer simulation is carried out for the problems of SSVIDEs, this allow us to estimate the precision of the mess-less scheme based on operational matrices for wavelet and

orthogonal polynomial respectively. High accuracy of the result even in the case of smaller number of wavelet basis function compare to Bernstein polynomial is observed. The numerical scheme of fractional derivative order and non-linear problems are a topic further study.

References

[1] Amari S., Dynamics of pattern formation in lateral inhibition type neural fields, Biological Cybernetics 1977; 27: 77-87.

[2] Gutkin, B., Pinto, D. and Ermentrout B. Mathematical neuroscience: from neurons to circuits to systems, J. Physiol. Paris 2003; 97: 209-219.

[3] Vineet K. Singh, Om P. Singh, and Rajesh K. Pandey, Almost Bernstein Operational Matrix Method for Solving System of Volterra Integral Equations of Convolution Type, Nonlinear Science Letters A, 2010; 1: 201-206.

[4] O. P Singh, V. K. Singh, and R. K. Pandey, A new stable algorithm for Abel inversion using Bernstein polynomials, International Journal of Nonlinear Sciences and Numerical Simulation 2009; 10: 891-896.

[5] K. Maleknejad and F. Mirzaee, Solving linear integro-differential equations system by using rationalized Haar functions method, Int. J. Computer math.2003: 1-9.

[6] K. Maleknejad and M. Tavassoli Kajani, Solving linear integro-differential equation system by Galerkin methods with hybrid functions, Appl. Math. Comput. 2004 ; 159: 603-612.

[7] K. Maleknejad and M. Shahrezaee, Using Runge-Kutta method for numerical solution of the system of Volterra integral equation, Appl. Math. Comput.2004; 149: 399-410.

[8] K. Maleknejad and A. Salimi Shamloo, Numerical solution of singular Volterra integral equations system of convolution type by using operational matrices, Appl. Math. Comput. 2008; 195: 500-505.

[9] Pinto, D. and Ermentrout, B., Spatially structured activity in synaptically coupled neuronal networks: I. traveling fronts and pulses, SIAM J. Appl. Math 2001; 62 :206-225

[10] Pinto, D. and Ermentrout, B. Spatially structured activity in synaptically coupled neuronal networks: II. lateral inhibition and standing pulses, SIAM J. Appl. Math 2001; 62: 226-243.

[11] Wilson, H. R. and Cowan, J. D., Excitatory and inhibitory interactions in localized populations of model neurons, Biophys. j. 1972; 12: 1-24.

[12] Wilson, H. R. and Cowan, J. D., A mathematical theory of the functional dynamics of control and thalamic nervous tissue, Kybernetik 1973; 13: 55-80.

[13] A.K. Singh, V. K. Singh, and O. P. Singh, The Betnstein operational matrix of integration. Appl. Math. Sci.2009; 3: 2427-2436.

[14] O. P. Singh, V. K. Singh, and R. K. Pandey, A stable numerical inversion of Abel's integral equation using almost Betnstein operational matrix, J. Quant. Spectrosc. Radiat. Transfer 2010; 111: 245-252.

[15] Vineet K. Singh, and E. B. Postnikov, Operational matrix approach for solution of integro-differential equations arising in theory of anomalous relaxation processes in vicinity of singular point, Appl. Math. Modell 2013; 37: 6609-6616.

[16] S.A. Yousefi, Numerical solution of Abel's integral equation by using Legendre wavelets, Appl. Math. Comput.2006;175:574–580.

[17] M. Razzaghi, S. Yousefi, The Legendre wavelets operational matrix of integration, Int. J. Syst. Sci.2011; 32: 495–502.

[18] Richard V. Kadison, Zhe Liu, The Heisenberg Relation - Mathematical, Symmetry, Integrability and Geometry: Methods and applications, 2014; 10: 009-40.